THE JOURNAL OF PHYSICAL CHEMISTRY B

Article

pubs.acs.org/JPCB

Nanoconfinement of Water Layers in Lamellar Structures Prepared in the Presence and Absence of Organic Solvent

Dipanwita De,[†] Manas Sajjan,[†] Janaky Narayanan,[‡] Jayesh R. Bellare,[‡] and Anindya Datta*,[†]

[†]Department of Chemistry and [‡]Department of Chemical Engineering, Indian Institute of Technology Bombay, Powai, Mumbai 400 076, India

Supporting Information

ABSTRACT: An attempt is made to draw a line of comparison between the extent of rigidity of the hydration layers bound to the interfacial region of lamellar structures of Aerosol OT (AOT, sodium bis(2-ethylhexyl) sulfosuccinate) in water, in the presence and absence of an organic solvent using POM, SAXS, cryo-TEM, and time-resolved fluorescence spectroscopy. These systems are ternary mixtures of AOT, water, and *n*-heptane containing lamellar structures in an aqueous layer at higher w_0 values (w_0 = 300 and 150) and a binary solution of 20 and 50% AOT in neat water (w/w). The solvation shells residing at the vicinity of these lamellar structures are monitored using two different coumarin probes (C153 and C500). It is intended to envisage a comparative solvation dynamics study of the restricted aqueous region confined in lamellar structures formed in ternary mixture and binary solution. Though steady state measurements show a similar microenvironment probed by the fluorophores in lamellar structures formed in the two different aqueous phases, temporal evolution of the solvent correlation function $C(t)$ unveils the existence of lamellar structures with different degrees of confinement of water layers in these two systems. A slower relaxation of the restricted aqueous region in lamellar structures of binary solution signifies the presence of more rigid interfacially bound water layers at the lamellar interface than in the ternary mixture having a similar weight percentage of AOT in water. The present investigation concludes that the lamellar structures formed under two different conditions provide a similar hydrophobic environment with different extents of localized water populations at the lamellar interface as manifested by the solvent relaxation time in agreement with SAXS and cryo-TEM images.

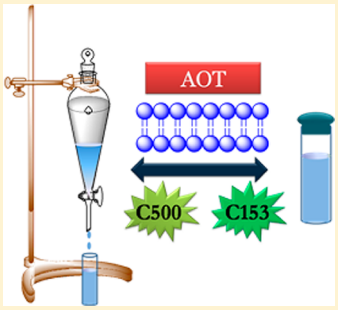

INTRODUCTION

In recent times, there has been a significant amount of interest in organized assemblies like micelles, reverse micelles, lamellar structures, vesicles, polymer−surfactant aggregates, and proteins.[1−4] The shape and size of these assemblies are governed by several covalent, electrostatic, and van der Waals forces which is known to tune the connectivity of water channels in these microenvironments.[5−7] The water in the vicinity of interfaces of these assemblies, called bound water, suffers loss of some degrees of freedom and thus exhibits widely different properties than bulk water. This modified aqueous phase is probed conveniently by fluorophores.[8−10] The occurrence of bound as well as free water in these systems gives rise to multimodal relaxation involving vastly different relaxation times ranging from femtoseconds to a few hundred picoseconds.[11−13] Careful study of the dynamics of interfacial bound water has been shown to reveal intricate detail about biological and biomimetic systems.[10,13−15]

The present article focuses on lamellar structures formed in the aqueous solutions of the surfactant Aerosol OT (AOT, sodium bis(2-ethylhexyl) sulfosuccinate) (Scheme 1).[6,16−18] AOT does not form normal micelles in water, as its shape can be approximated to be a wedge, with the thin end toward the sulfonate headgroup. However, this geometry favors the formation of lamellar structures.[19] In recent times, attempts have been made to elucidate the interlamellar distance and hydration structure of interfacial water in AOT lamellar structures using X-ray diffraction,[20] infrared spectroscopy,[20,21] NMR, and differential scanning calorimetry.[22,23] Infrared investigation of lamellar structures formed using AOT in water reveals the existence of three types of water populations, viz., (a) network water (NW), (b) intermediate water (IW), and (c) multimer water (MW).[20] Network water (NW)

Scheme 1. Molecular Structures of AOT, Coumarin 153 (C153), and Coumrin 500 (C500)

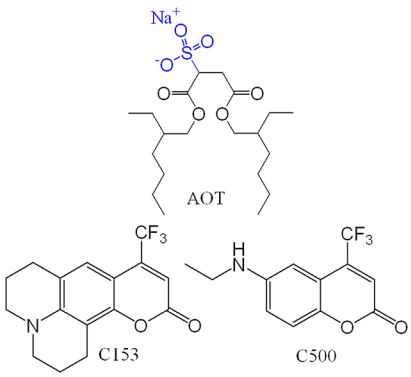

Received: July 2, 2012
Published: December 17, 2012

dx.doi.org/10.1021/jp310371a | J. Phys. Chem. B 2013, 117, 2106−2112

molecules are bound to four other water molecules each, while three neighboring water molecules are hydrogen bonded to each intermediate water (IW) molecule. Each multimer water (MW) molecule is hydrogen bonded to two other water molecules. The thickness of the hydration layer is considered to be the key factor that determines the relative proportion of these three kinds of water populations.[20] A system like this is of potential interest for the study of solvation dynamics, which has been explored in great detail in three-dimensional surfactant aggregates like micelles and reverse micelles, using fluorescence spectroscopy.[9,10,24] However, to the best of our knowledge, there is only one such study in two-dimensional lamellar aggregates of surfactants, that establishes an overall slower relaxation dynamics of water confined in AOT lamellar micelle as compared to reverse micelle water pool having identical water to surfactant ratio.[25] It is surprising that more such studies have not been performed so far. The solvation dynamics in these systems promises to be interesting, as the two-dimensional shape of lamellar aggregates alters the degree of hydration and connectivity of the confined water.

With this motivation, we have attempted to investigate solvation dynamics in lamellar structures of AOT. These structures have been prepared in two ways. In one method, aqueous solutions of AOT have been prepared following the protocol reported earlier.[25] In the other method, ternary mixtures of AOT, water, and *n*-heptane have been allowed to stand and the lower, aqueous layer has been isolated. This layer contains lamellar structures of AOT. The interest in investigating the lamellar structures of AOT prepared in the second method has arisen from the observation reported earlier by our group, on the formation of silica nanodisks from this layer, through the mediation of lamellar structures as templates.[26] One of the principal motivations of the present study is to understand whether the dynamics of solvent relaxation is the same in the lamellar structures prepared by the two methods or not. Two different fluorophores, namely, coumarin 153 (C153) and coumarin 500 (C500) (Scheme 1), have been used in this study. Though both the coumarin dyes have similar structures, the amine group in C500 is acyclic, while it is cyclized in C153. The ground state dipole moments of both of the dyes are almost the same.[27,28] On excitation, the dipole moment of C153 suffers a significant change of 8−10 D depending upon the solvent.[27] A relatively smaller dipole moment change of 2−4 D is reported for C500.[28] The effect of the difference in the change in dipole moment, on solvation dynamics in lamellar structures, has been discussed in the present article.

MATERIALS AND METHODS

Aerosol OT (AOT, sodium bis(2-ethylhexyl) sulfosuccinate) obtained from Sigma Aldrich (98% pure) is dried and purified using the literature method.[29] HPLC grade *n*-heptane (98% pure) from Spectrochem, Mumbai, India, is dried and distilled prior to use. C153 and C500 from Radiant Dyes have been used as received. All aqueous solutions have been prepared using Millipore water. Binary solutions are prepared in plastic cuvettes obtained from Brookhaven Instruments and Services, Mumbai, India.

Preparation of Ternary Mixtures. Ternary mixtures of w_0, a measure of the molar ratio of water to AOT, of 150 and 300 are prepared with required weight of AOT dissolved in *n*-heptane and aqueous solution of coumarin in separating funnels and shaken thoroughly to facilitate the dissolution of the solute. Thereafter, the separating funnels are left undisturbed for 1−2 days so as to attain equilibrium and complete phase separation. The lower aqueous layer containing the lamellar structures is then carefully isolated for subsequent measurements. The upper oil-rich heptane layer is discarded. The net concentration of AOT is maintained at 40.5 mM throughout.

Preparation of Binary Solutions. Binary solutions are prepared following the procedure reported elsewhere.[25] 20 and 50% (w/w) solutions of AOT in water are prepared in properly sealed plastic cuvettes containing a weighed amount of AOT in a desired volume of water. The cuvettes are then heated to 50 °C followed by back and forth centrifugation. The binary solutions thereby formed are allowed to equilibrate at room temperature before carrying out any spectroscopic measurement.

Characterization of the Lamellar Structures. Polarization optical micrograph (POM) images are collected using a Leica DM4500 P microscope equipped with a Leica DFC 420 camera. SAXS experiments are performed in line collimation, in a modified Kratky camera (SAXSess Anton Paar, Austria) using Cu Kα as incident radiation (λ = 1.542 Å). The sample to detector distance is maintained at 26.5 cm. After acquisition of scattering intensities in a capillary tube over a period of 20 min at 25 °C on a two-dimensional position sensitive imaging plate, intensities are integrated over a linear profile to convert into one-dimensional scattering data of scattering intensity $I(q)$ vs scattering wave vector q ($q = 2\pi/d = 4\pi \sin\theta/\lambda$). Solvent correction using Millipore water is done to obtain the scattering intensity of lamellar structures in arbitrary scale. The observed scattering pattern originates from the (001) plane.[20] The cryo-TEM experiments are performed by blotting the appropriately diluted sample on a holey carbon grid of 200 mesh and then subsequently plunged in a VITROBOT (FEI) at room temperature. The sample is then transferred to JEM-2100HRTEM electron microscope provisioned with Gatan cold stage. Then, it is examined under an acceleration voltage of 200 kV in the conventionally operated TEM mode. The working temperature here is maintained at −173 °C. Images are recorded using a Gatan CCD Orius Camera.

Electronic Absorption and Fluorescence. The absorption and emission spectra are recorded with a JASCO V530 UV−vis spectrophotometer and a Varian Cary Eclipse spectrofluorimeter, respectively. Excitation wavelengths of 375, 400, and 440 nm have been used to record the fluorescence spectra with excitation and emission slits at 5 nm. A picosecond pulsed diode laser based time correlated single photon counting (TCSPC) instrument from IBH (United Kingdom) is used to collect time-resolved decays at different wavelengths, with the emission polarizer set at a magic angle of 54.7° with respect to the polarization of the incident light. Pulsed laser sources of 440 and 402 nm with 250 ps fwhm are used having a resolution of 14 ps/channel. The decay traces are fitted to a sum of exponential functions, as shown below using the iterative reconvolution technique by IBH DAS 6.2 data analysis software.[30,31]

$$I(\lambda, t) = I_0(\lambda) \sum_i a_i e^{-t/\tau_i} \quad (1)$$

Here $I(\lambda, t)$ is the fluorescence intensity at an emission wavelength of λ at a time t after excitation. $I_0(\lambda)$ is the fluorescence intensity at an emission wavelength of λ at time zero. τ_i and a_i are the lifetime and amplitude of the ith

dx.doi.org/10.1021/jp310371a | J. Phys. Chem. B 2013, 117, 2106−2112

component, respectively. In order to construct time-resolved emission spectra (TRES), fluorescence decays are collected at intervals of 10 nm throughout the range of emission spectrum and the following equation is used to generate the emission spectra at different values of t after excitation, using the amplitudes, lifetimes, and steady state intensity, $I_{SS}(\lambda)$, at the same wavelength λ.[32−34]

$$I(\lambda, t) = I_{SS}(\lambda)\frac{\sum_i a_i e^{-t/\tau_i}}{\sum_i a_i \tau_i} \quad (2)$$

TRES are generated for t = 0−10 ns. The solvent correlation function $C(t)$ generated using the emission maxima of respective TRES has the following expression.[11]

$$C(t) = \frac{\nu(t) - \nu(\infty)}{\nu(0) - \nu(\infty)} \quad (3)$$

Here $\nu(0)$, $\nu(t)$, and $\nu(\infty)$ are emission maxima (in cm^{-1}) at time zero, t, and infinity, when no further solvation occurs, respectively. The $C(t)$ curve generated against time is fitted to a biexponential decay function with time constants, τ_i, and corresponding amplitudes, A_i.

RESULTS AND DISCUSSION

Structural Characterization of Lamellar Structures. POM images acquired for the aqueous layer of a ternary mixture and binary solution confirm the presence of lamellar structures (Figure S1 of Supporting Information). SAXS of the AOT bilayer formed in the aqueous solution isolated from a lower layer of the ternary mixture exhibits a similar diffraction pattern for the two different concentrations of AOT used (Figure 1a). The plot of scattering intensities against scattering wave vector q exhibits a maximum at q = 0.37 nm^{-1}. This corresponds to a bilayer thickness (d) of 16.97 nm. The thickness of the water layer is extracted by subtracting 1.90 nm, which is the length of two nonpenetrating AOT molecules, from the bilayer thickness.[20] This calculation yields a water layer thickness of ∼15.1 nm in the ternary mixture. A thickness of 9 nm is estimated for lamellar structures formed in 20% aqueous AOT solution, from X-ray diffraction data presented in an earlier report.[20] Thus, the lamellar structures in the aqueous layer of the ternary mixture are found to have a hydration layer that is less restricted than that in lamellar structures formed in binary solutions. A direct support for this contention is obtained using cryo-TEM. The TEM image clearly brings out the multilamellar nature of the structures formed by AOT in the ternary mixture (Figure 1b). The thickness of water layers in this structure is found to be ∼20−25 nm.

Steady State Spectra in Lamellar Structures Formed in the Aqueous Layer of Ternary Mixtures. Absorption spectra of C153 and C500 in water show distinct maxima at 432 and 395 nm, respectively.[35,36] Blue shifted structured absorption spectra with maxima around 417 and 387 nm are observed for C153 and C500, respectively, in ternary mixtures of w_0 = 300 and 150 (Figure 2). The structured absorption band in lamellar structures formed in the water rich layer of ternary mixtures is similar to that observed in n-heptane (Figure S2 of the Supporting Information).[27,36] This indicates a nonpolar environment experienced by the fluorophore in these lamellar structures. C153 and C500 exhibit emission maxima at 552 and 510 nm, respectively, in aqueous solution (Figure 2). Fluorescence spectra of the C153 and C500 undergo a blue shift in the presence of lamellar structures with emission

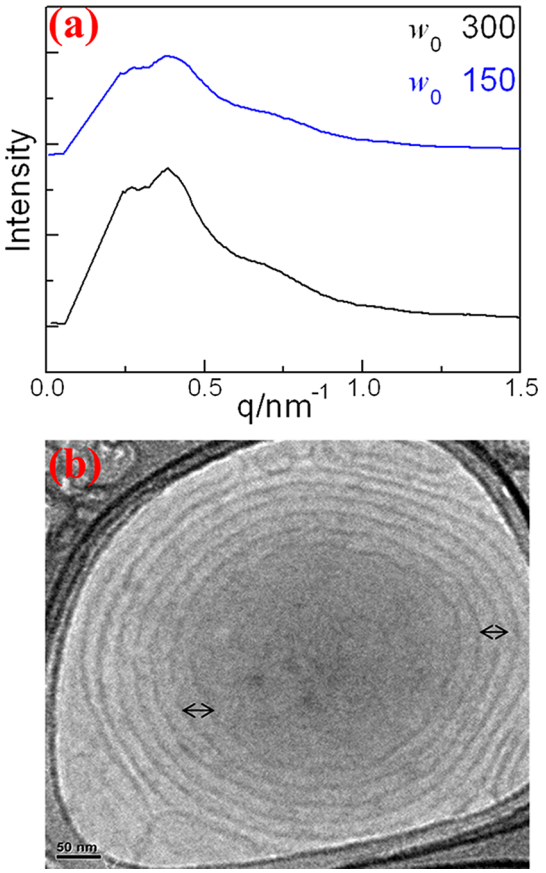

Figure 1. (a) Small angle X-ray diffraction patterns of aqueous layers isolated from a ternary mixture of w_0 = 300 and 150. (b) Cryo-TEM image obtained for an aqueous layer of w_0 = 300. The arrow (↔) indicates the thickness of the aqueous layer sandwiched between the AOT bilayers.

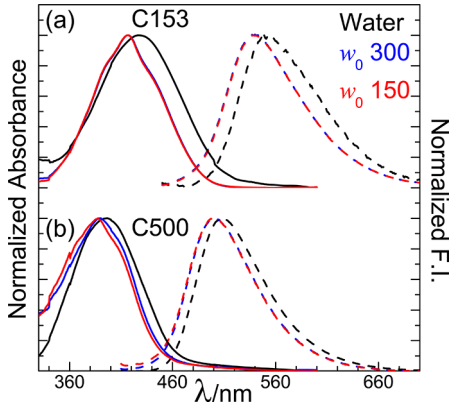

Figure 2. Normalized absorption (solid line) and emission spectra (dashed line) of (a) C153 and (b) C500 in water and an aqueous layer of a ternary mixture of w_0 = 300 and 150. The emission spectra are recorded at λ_{ex} = 440 and 400 nm for C153 and C500, respectively.

maxima at 537 and 500 nm, respectively. A greater change in the dipole moment in the excited state[27] substantiates a more pronounced blue shift for C153 as compared to C500. Upon excitation at the blue edge of the absorption band of the dyes in w_0 = 300 and 150, an additional structured emission band with small intensity is observed. The maxima of this band occur at ca. 440 nm for C153 and at 420 nm for C500 (Figure S2 of the Supporting Information). These structured emission bands can

dx.doi.org/10.1021/jp310371a | J. Phys. Chem. B 2013, 117, 2106−2112

be ascribed to the probes in a nonpolar environment, as the spectral features mimic those observed in *n*-heptane. The emission spectra at two w_0 values are found to be identical. In order to explain this, the weight percentages of AOT in water are determined, under the consideration of complete partitioning of AOT in water in a ternary mixture as done in our previous study.[26] The weight percentage of AOT in w_0 = 300 is estimated to be 8%, and in w_0 = 150, it is 16.5%. Prouzet and co-workers in their studies using the X-ray diffraction technique confirmed the absence of lamellar structures at 5% AOT in water solution.[20] Lamellar structures are found to form at and above 10% AOT in water which is close to the calculated weight percentage for w_0 = 300 of the ternary mixture. Thus, one may infer that the nature of the lamellar structures is the same in both w_0 values, with the number of such aggregates being lesser at w_0 = 300. This is evident from crossed polarization optical micrographs of the water rich layer as well (Figure S1a,b of the Supporting Information).

Steady State Spectra in Lamellar Structures Formed in the Binary Solutions. The absorption spectra for C153 and C500 undergo small changes upon incorporation in lamellar structures formed in binary solution of AOT in water (Figure 3). Excitation spectra for both the dyes in aqueous

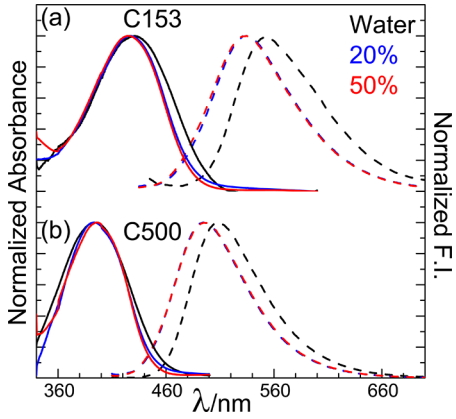

Figure 3. Normalized absorption (solid line) and emission spectra (dashed line) of (a) C153 and (b) C500 in water and 20 and 50% AOT in water (w/w). The emission spectra are recorded at λ_{ex} = 400 nm.

solutions in the absence and presence of lamellar structures indicate the existence of a single emissive species for each coumarin dye (Figure S3 of the Supporting Information). Fluorescence spectra undergo more pronounced changes. Blue shifts of 20 and 13 nm are observed for C153 and C500, respectively, as compared to the values in water, marking the incorporation of the two fluorophores in lamellar structures (Figure 3). Unlike ternary mixtures, the emission spectra of both of the probes in a binary mixture show a single emission band at 535 nm for C153 and 495 nm for C500. This signifies that the hydrophobic regions of the lamellar structures obtained from the binary solutions are less apolar than those prepared from ternary mixtures. It is possible that the lamellar structures trap a significant amount of *n*-heptane during its formation in ternary mixture and, thus, the fluorophores exhibit structured absorption and emission spectra, typical of *n*-heptane solutions, in these lamellar structures. This kind of spectral feature is absent in lamellar structures prepared from binary solutions, in which such a possibility does not exist. It may be noted here that the two coumarin dyes have identical emission spectra for 20 and 50% AOT in water, suggesting the presence of similar lamellar structures for the two compositions. This contention is in line with the images of polarization optical microscopy (POM) (Figure S1c,d of the Supporting Information). An inspection of the emission spectra of the corresponding dyes in lamellar structures formed in a ternary mixture and a binary solution in water reveals the presence of similar lamellar structures in both of the systems. Thus, coumarin dyes, upon incorporation in lamellar structures formed in the water layer of a ternary mixture, seem to experience a similar microenvironment as those formed in binary solutions.

Time-Resolved Fluorescence Studies in Lamellar Structures Formed in the Aqueous Layer of Ternary Mixtures. Wavelength dependent decays are observed for C153 and C500 upon excitation at λ_{ex} = 440 and 402 nm, respectively. The decays collected at different wavelengths across the emission spectra are fitted to biexponential functions. The fluorescence transients are marked by a fast decay at the blue edge and a corresponding rise at the red edge of the spectrum (Figure 4 and Figure S4 of the Supporting

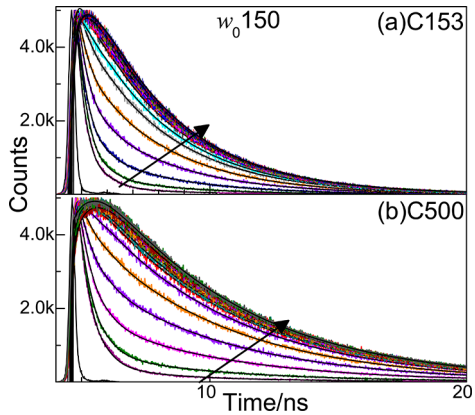

Figure 4. Fluorescence transients of (a) C153 (λ_{ex} = 440 nm) and (b) C500 (λ_{ex} = 402 nm) at different emission wavelengths recorded across the respective emission spectrum shown by the arrow in an aqueous layer of w_0 = 150 of a ternary mixture.

Information). The short lifetimes in the blue edge are 400 and 550 ps for C153 and C500, respectively, while the long components are around 3.3 and 5.5 ns, respectively (Table 1 and Table S1 of the Supporting Information). The rise times at the red end of the spectra are 460−500 ps for C153 and 550−650 ps for C500. The emission spectra generated at different time intervals ranging from 0 ns to 10 ns using eq 2 exhibit a time dependent Stokes shift (TDSS) (insets of Figure 5 and Figure S5 of the Supporting Information). The slow temporal evolution of the emission spectra for w_0 = 300 and 150 is ascribed to slow solvation of the probes in the aqueous phase.

The solvent correlation function $C(t)$ curves obtained for the coumarin dyes using eq 3 are fitted to a biexponential decay function following a two-component core−shell model proposed by Pal and co-workers[25] (Figure 5). The two components arise due to slow relaxation of network water (bulk-like) and intermediate water (interfacially bound), as defined by Prouzet and co-workers.[20] The network water at the vicinity of the dyes relaxes faster with a time constant of around 0.28 ns (Table 2). AOT being an anionic surfactant forms lamellar aggregates with their polar head projected outward,

dx.doi.org/10.1021/jp310371a | J. Phys. Chem. B 2013, 117, 2106−2112

Table 1. Time-Resolved Decay Parameters of C153 and C500 in an Aqueous Layer of a Ternary Mixture of w_0 = 150 and 20% AOT in Water at λ_{ex} = 440 and 402 nm, Respectively[a]

dye	λ_{em} (nm)	τ_1 (ns)	τ_2 (ns)	A_1	A_2	χ^2
C153, w_0 = 150	480	0.39	2.88	0.91	0.09	1.20
	510	0.42	3.27	0.66	0.34	1.08
	530		3.31		1.00	1.04
	560	0.46	3.32	−0.23	1.23	1.00
	600	0.46	3.32	−0.42	1.42	1.00
	640	0.46	3.33	−0.53	1.53	1.00
C500, w_0 = 150	450	0.55	5.16	0.88	0.12	1.01
	470	0.57	5.37	0.51	0.49	1.11
	490		5.41		1.00	1.03
	520	0.56	5.48	−0.33	1.33	1.02
	560	0.58	5.46	−0.58	1.58	1.08
	600	0.65	5.48	−0.72	1.72	1.08
C153, 20%	480	0.53	2.79	0.77	0.23	1.19
	510	0.61	3.57	0.34	0.66	1.04
	530		3.74		1.00	1.05
	560	0.70	3.73	−0.40	1.40	1.00
	600	0.71	3.74	−0.77	1.77	1.06
	640	0.73	3.77	−0.96	1.96	1.03
C500, 20%	450	0.65	4.36	0.68	0.32	1.20
	470	0.76	5.31	0.36	0.64	1.03
	490		5.60		1.00	1.02
	520	0.84	5.72	−0.30	1.30	1.00
	560	0.84	5.78	−0.55	1.55	1.05
	600	0.87	5.78	−0.66	1.66	1.03

[a]The decays are fitted to biexponential functions: $I(t) = I(0)[A_1 \exp(-t/\tau_1) + A_2 \exp(-t/\tau_2)]$. Here $\tau_1$and τ_2 are the lifetimes having amplitudes A_1 and A_2, respectively.

and neighboring water molecules adhere onto these head groups through suitable dipole−dipole interactions. These molecules, therefore, lack some degrees of freedom, and in order to relax, they have to disrupt the existing interactions, which are energetically costly and thereby slow. This interfacially bound intermediate water is found to relax at a much slower rate with time constants of around 0.85 ns (Table 2). The average lifetimes, τ_{avg}, are found to be independent of the water to surfactant ratio and the intrinsic properties of the fluorophore. This rationalizes the presence of similar types of water populations around the probe at both w_0 values.

Time-Resolved Fluorescence Studies in Lamellar Structures Formed in the Binary Solutions. Fluorescence decays recorded at λ_{ex} = 402 nm display substantial wavelength dependence as in ternary mixtures. A biexponential fit to the fluorescence transients shows a fast decay and a rise time at the blue and red edge, respectively (Figure 6 and Figure S6 of the Supporting Information). The fluorescence decays at a particular wavelength are different for C153 and C500. The fast decays at shorter wavelengths have time constants of 530−700 ps and 3.7 ns for C153, while the same for C500 are 650−950 ps and around 5.5 ns (Table 1 and Table S1 of the Supporting Information). Rise times of 660−730 ps for C153 and 830−940 ps for C500 are observed at the red end of the emission spectra for 20 and 50% AOT in water. Though the long component of C153 and C500 in binary solutions is consistent with that in ternary mixtures, the short component at the blue end and the rise time at the red end are distinctly different (Table 1 and Table S1 of the Supporting

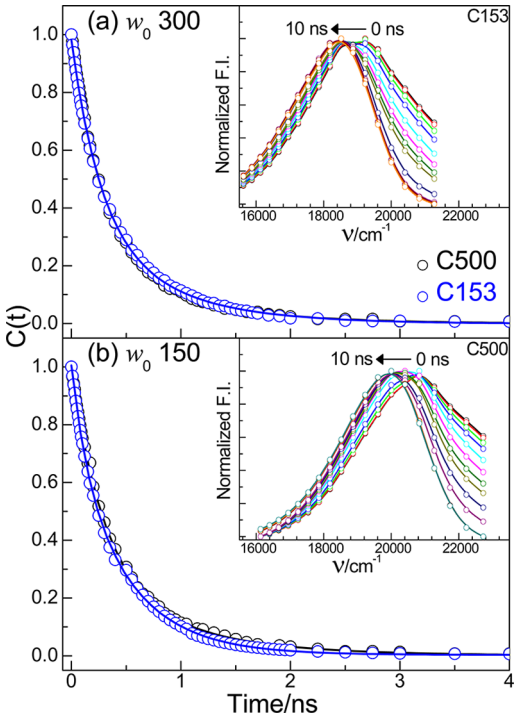

Figure 5. Solvent correlation function $C(t)$ of C153 (blue circle) and C500 (black circle) at λ_{ex} = 440 and 402 nm, respectively, in lamellar structures of (a) w_0 = 300 and (b) w_0 = 150 in a ternary mixture. Temporal evolution of emission spectra exhibiting time dependent Stokes shift (TDSS) for C153 and C500 in an aqueous layer of w_0 = 150 of a ternary mixture are shown as insets. The arrows indicate an increase in time from 0 to 10 ns. The times are 0, 0.01, 0.05, 0.1, 0.2, 0.3, 0.4, 0.5, 1, 2, 3, 5, and 10 ns for both C153 and C500.

Table 2. Fitted Biexponential Decay Parameters of the Solvation Correlation Function $C(t)$ Generated for C153 and C500 in an Aqueous Layer of a Ternary Mixture and Binary Solution[a]

composition	dye	τ_1 (ns)	τ_2 (ns)	A_1	A_2	τ_{avg} (ns)	R^2
w_0 = 300	C153	0.26	0.79	0.65	0.35	0.44	0.99
	C500	0.28	0.87	0.73	0.27	0.44	0.99
w_0 = 150	C153	0.28	0.85	0.72	0.28	0.44	0.99
	C500	0.30	0.89	0.71	0.29	0.47	0.99
20%	C153	0.57	1.21	0.77	0.23	0.72	0.99
	C500	0.53	1.52	0.59	0.41	0.93	0.99
50%	C153	0.49	1.22	0.62	0.38	0.76	0.99
	C500	0.68	2.10	0.71	0.29	1.10	0.99

[a]τ_{avg} is the average lifetime given by $\tau_1A_1 + \tau_2A_2$, and R^2 determines the goodness of fit.

Information). The short lifetime and the rise time of both the probes are longer in binary solution. This suggests a comparatively slower solvent relaxation of the water populations at the vicinity of lamellar structures formed in binary solution. Like the ternary mixture, TRES generated for the probes in 20 and 50% aqueous solutions of AOT show a time dependent Stokes shift (TDSS) in these lamellar structures as well (insets of Figure 7 and Figure S7 of the Supporting Information). A Stokes shift of 1063 cm^{-1} is observed for C153 and 920 cm^{-1} for C500 in 50% AOT in water solution. This value of Stokes shift for C500 in 50% AOT solution is in congruence with an earlier report on C500 in 40% AOT in water.[25]

dx.doi.org/10.1021/jp310371a | J. Phys. Chem. B 2013, 117, 2106−2112

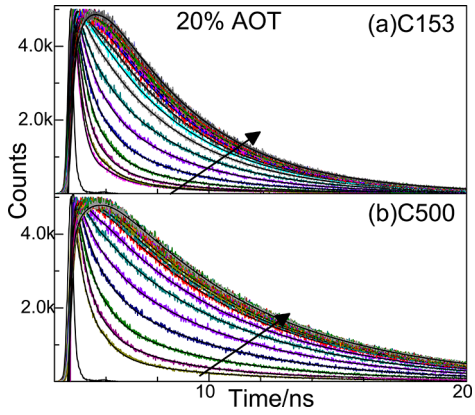

Figure 6. Fluorescence transients of (a) C153 and (b) C500 at different emission wavelengths recorded across the respective emission spectrum shown by the arrow in 20% AOT in water (λ_{ex} = 402 nm).

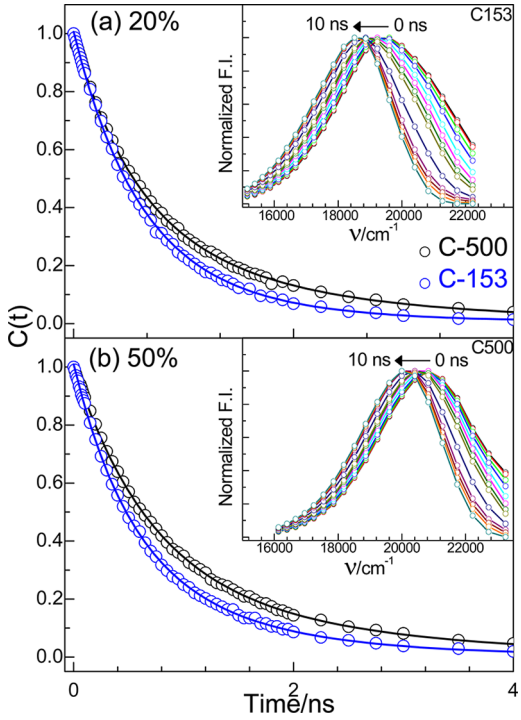

Figure 7. Solvent correlation function $C(t)$ of C153 (blue circles) and C500 (black circles) in lamellar structures of (a) 20% and (b) 50% AOT in water. Temporal evolution of emission spectra exhibiting time dependent Stokes shift (TDSS) for C153 and C500 in 20% AOT in water are shown as insets. The arrows indicate an increase in time from 0 to 10 ns. The times are 0, 0.01, 0.05, 0.1, 0.2, 0.3, 0.4, 0.5, 1, 2, 3, 5, and 10 ns for both C153 and C500.

The time evolution of the correlation function $C(t)$ obtained for the coumarin dyes in binary solution is fitted to a biexponential decay function as done for ternary mixtures (Figure 7). The bulk-like network water population responds very quickly to the generated dipole in the excited state and shows a time constant of 0.57−0.68 ns depending upon the dye and the composition of AOT in water, while a more restricted intermediate water relaxes slowly with time constants varying from 1.21 to 2.10 ns (Table 2). A comparison between the τ_{avg} values of the two coumarin probes in a given percentage of AOT in water reveals an interesting aspect. For 50% solutions of AOT in water, the τ_{avg} value of C153 is 0.76 ns which is lower than 1.10 ns for C500. This observation holds for 20% AOT in water as well and can be rationalized on the basis of the prominent difference in the augmentation of the dipole moment on excitation of these two probes.[37] The increase in dipole moment in C153 is around 4 times more than that in C500, the ground state dipole moment of the two dyes being comparable.[27,28] Therefore, C153 creates a stronger electric field and consequently makes water molecules orient faster than by C500. The difference in the change of electric field exerted by the dye is less pronounced for the shorter time constant than for the longer one, as the bulk-like network water is free and can relax promptly under any electric field, whether strong or weak; it is the restricted interfacially bound water that can sense the difference. However, no appreciable change in the overall decay of the correlation function $C(t)$ for a given coumarin dye signifies a similar solvation shell is experienced by the fluorophore in lamellar aggregates of 20 and 50% AOT in water (Figure S8 of the Supporting Information). It may be noted here that, unlike binary solutions, the relaxation of the interfacial hydration layer in lamellar structures of ternary mixtures is much faster, an observation which is in line with SAXS and cryo-TEM measurements. This strongly supports that the hydration layer confined within the lamellar structures formed in a ternary mixture is much more flexible, allowing the water molecules to orient promptly around the fluorophore.

CONCLUSION

The time dependent response of the aqueous phase confined within lamellar structures of AOT prepared in two different systems is investigated using time-resolved fluorescence spectroscopy. The results are interpreted in terms of relaxation dynamics of the two different populations of water residing at the lamellar interface. The lamellar structures formed in a ternary mixture at different water to surfactant ratios are found to provide a similar nonpolar microenvironment to the coumarin probes as in a binary solution of comparable weight percentage of AOT in water. This clearly indicates that the inherent nature of the lamellar structures, existing in these two different systems, is similar. However, the time dependent relaxation dynamics of the solvent upon excitation of the probes exhibits a distinctly different relaxation time constant. Solvation of interfacial water layers with a τ_{avg} value of 0.72−1.10 ns in binary solution is more retarded than in a ternary mixture with a τ_{avg} value of 0.44 ns. This is attributed to the higher degree of restriction of the aqueous phase in lamellar structures of binary solution as suggested by SAXS and cryo-TEM measurements. Furthermore, the water populations at the vicinity of lamellar structures of binary solution are localized to an extent that its relaxation dynamics is affected by the change in dipole moment of the probe upon excitation. This is manifested by a slower solvation experienced by C500 than C153 in these structures for the same weight percentage of AOT. In contrast, the solvation dynamics of C153 and C500 in the hydration layer bound to the lamellar interface of a ternary mixture is independent of the difference in augmentation of the excited state dipole moment of the two probes. An average relaxation time of 0.45 ns is reported[38] for C153 incorporated in sodium dodecyl sulfate (SDS) micelles having a negatively charged interface similar to that of AOT. Similarly, C500 in AOT reverse micelle of w_0 = 46 which is equivalent to 35% AOT in water is reported to exhibit an average relaxation lifetime of 0.48 ns.[25] The τ_{avg} values in SDS micelles and AOT reverse micelles are in parity with our observation of average

dx.doi.org/10.1021/jp310371a | J. Phys. Chem. B 2013, 117, 2106−2112

lifetime for C500 and C153 in lamellar structures of a ternary mixture. This indicates that lamellar structures formed in a ternary mixture possess a similar confinement of hydration layers as in SDS micelles and AOT reverse micelles, regardless of the dimensionality. Thus, irrespective of the inherent nature of the probe, it is the degree of hydration confined within these lamellar structures which governs the relaxation dynamics of the interfacial water structures.

■ ASSOCIATED CONTENT

Supporting Information

Additional POM images, absorption spectra, fluorescence spectra, time-resolved decays, and table of decay parameters. This material is available free of charge via the Internet at http://pubs.acs.org.

■ AUTHOR INFORMATION

Corresponding Author

*Phone: +91 22 2576 7149. Fax: +91 22 2570 3480. E-mail: anindya@chem.iitb.ac.in.

Notes

The authors declare no competing financial interest.

■ ACKNOWLEDGMENTS

This work is supported by the SERC., DST. D.D. thanks CSIR for a Senior Research Fellowship. The POM images are recorded in the Department of Earth Sciences, IIT Bombay, with help from Mr. Swarnava Chakraborty, Mr. Dhiren Kumar Ruidas, and Prof. Santanu Banerjee.

■ REFERENCES

(1) Bhattacharyya, K. *Acc. Chem. Res.* **2003**, *36*, 95−101.
(2) Haldar, A.; Sen, P.; Burman, A. D.; Bhattacharyya, K. *Langmuir* **2004**, *20*, 653−657.
(3) Burai, T. N.; Datta, A. *J. Phys. Chem. B* **2009**, *113*, 15901−15906.
(4) Goyal, P. S.; Aswal, V. K. *Curr. Sci.* **2001**, *80*, 972−979.
(5) Lee, M.; Cho, B.-K.; Zin, W.-C. *Acc. Chem. Res.* **2001**, *101*, 3869−3692.
(6) Pileni, M. P. *Langmuir* **1997**, *13*, 3266−3276.
(7) Petit, C.; Lixon, P.; Pileni, M. P. *Langmuir* **1991**, *7*, 2620−2625.
(8) Hazra, P.; Sarkar, N. *Phys. Chem. Chem. Phys.* **2002**, *4*, 1040−1045.
(9) Levinger, N. E.; Swafford, L. A. *Annu. Rev. Phys. Chem.* **2009**, *60*, 385−406.
(10) Bhattacharyya, K.; Bagchi, B. *J. Phys. Chem. A* **2000**, *104*, 10603−10613.
(11) Bagchi, B.; Jana, B. *Chem. Soc. Rev.* **2010**, *39*, 1936−1954.
(12) Das, S.; Datta, A.; Bhattacharyya, K. *J. Phys. Chem. A* **1997**, *101*, 3299−3304.
(13) Lundgren, J. S.; Heitz, M. P.; Bright, F. B. *Anal. Chem.* **1995**, *67*, 3775−3781.
(14) Banerjee, D.; Pal, S. K. *Chem. Phys. Lett.* **2008**, *451*, 237−242.
(15) Pal, N.; Verma, S. D.; Sen, S. *J. Am. Chem. Soc.* **2010**, *132*, 9277−9279.
(16) Satpati, A. K.; Kumbhakar, M.; Nath, S.; Pal, H. *ChemPhysChem* **2009**, *10*, 2966−2978.
(17) Pileni, M. P. *Langmuir* **2001**, *17*, 7476−7486.
(18) Pileni, M. P. *Nat. Mater.* **2003**, *2*, 145−150.
(19) Moroi, Y. *Micelles Theoretical and Applied Aspects*, 1st ed.; Springer: New York, 1992.
(20) Boissière, C.; Brubach, J. B.; Mermet, A.; de Marzi, G.; Bourgaux, C.; Prouzet, E.; Roy, P. *J. Phys. Chem. B* **2002**, *106*, 1032−1035.
(21) Moilanen, D. E.; Fenn, E. E.; Wong, D.; Fayer, M. D. *J. Am. Chem. Soc.* **2009**, *131*, 8318−8328.
(22) Casillas, N.; Puig, J. E.; Olayo, R.; Hart, T. J.; Franses, E. I. *Langmuir* **1989**, *5*, 384−389.
(23) Prouzet, E.; Brubach, J. -B.; Roy, P. *J. Phys. Chem. B* **2010**, *114*, 8081−8088.
(24) Shirota, H.; Tamoto, Y.; Segawa, H. *J. Phys. Chem. A* **2004**, *108*, 3244−3252.
(25) Verma, P. K.; Saha, R.; Mitra, R. K.; Pal, S. K. *Soft Matter* **2010**, *6*, 5971−5979.
(26) Banerjee, S.; Ghosh, H.; Datta, A. *J. Phys. Chem. C* **2011**, *115*, 19023−19027.
(27) Hazra, P.; Chakrabarty, D.; Sarkar, N. *Chem. Phys. Lett.* **2003**, *371*, 553−562.
(28) Nad, S.; Pal, H. *J. Phys. Chem. A* **2003**, *107*, 501−507.
(29) Maltra, A. N.; Elcke, H-F. *J. Phys. Chem.* **1981**, *85*, 2687−2691.
(30) Mukherjee, T. K.; Panda, D.; Datta, A. *J. Phys. Chem. B* **2005**, *109*, 18895−18901.
(31) Mishra, P. P.; Koner, A. L.; Datta, A. *Chem. Phys. Lett.* **2004**, *400*, 128−132.
(32) Detoma, R. P.; Brand, L. *Chem. Phys. Lett.* **1977**, *47*, 231−236.
(33) Koti, A. S. R.; Periasamy, N. *J. Chem. Phys.* **2001**, *115*, 7094−7099.
(34) Koti, A. S. R.; Krishna, M. M. G.; Periasamy, N. *J. Phys. Chem. A* **2001**, *105*, 1767−1771.
(35) Seth, D.; Sarkar, S.; Sarkar, N. *Langmuir* **2008**, *24*, 7085−7091.
(36) Das, K.; Jain, B.; Gupta, P. K. *Chem. Phys. Lett.* **2005**, *410*, 160−164.
(37) Maroncelli, M.; Fleming, G. R. *J. Chem. Phys.* **1988**, *89*, 5044−5069.
(38) Shirota, H.; Tamoto, Y.; Segawa, H. *J. Phys. Chem. A* **2004**, *108*, 3244−3252.